

FRCM retrofitting techniques for masonry walls: a literature review and some laboratory tests

Original

FRCM retrofitting techniques for masonry walls: a literature review and some laboratory tests / Cucuzza, R.; Domaneschi, M.; Camata, G.; Marano, G. C.; Formisano, A.; Brigante, D.. - In: PROCEDIA STRUCTURAL INTEGRITY. - ISSN 2452-3216. - 44:(2023), pp. 2190-2197. (19th ANIDIS Conference, Seismic Engineering in Italy Turin (ITA) 11-15 September 2022) [10.1016/j.prostr.2023.01.280].

Availability:

This version is available at: 11583/2982826 since: 2023-10-06T16:13:10Z

Publisher:

Elsevier

Published

DOI:10.1016/j.prostr.2023.01.280

Terms of use:

This article is made available under terms and conditions as specified in the corresponding bibliographic description in the repository

Publisher copyright

(Article begins on next page)

1 XIX ANIDIS Conference, Seismic Engineering in Italy

2 FRCM retrofitting techniques for masonry walls: a literature review
3 and some laboratory tests

4 Raffaele Cucuzza^{a,*}, Marco Domaneschi^a, Guido Camata^b, Giuseppe Carlo Marano^a,
5 Antonio Formisano^c and Domenico Brigante^d

6 ^aPolitecnico of Turin, Corso Duca degli Abruzzi 24, Turin (TO) 10129

7 ^bUniversità degli Studi "G.d'Annunzio" of Chieti-Pescara, Viale Piandaro 42, Pescara (PE) 66100

8 ^cUniversità fo Naples "Federico II", Piazzale Tecchio 80, Naples (NA) 80125

9 ^dOlympus-FRP Srl, Via Riviera Di Chiaia 118, Naples, 80122

10
11 **Abstract**

12 The experimental characterisation of externally bonded composite materials as strengthening solutions for masonry structures,
13 such as basalt textile reinforced mortar (BTRM) or fiber reinforced concrete (FRC), has been receiving increasing attention due
14 to their outstanding mechanical performance. Several studies have been demonstrated the efficiency of this retrofitting solution
15 for increasing the mechanical strength and the displacement capacity of masonry material.

16 In this paper the state-of-art of the most relevant achievements in the experimental investigations and numerical analysis of
17 retrofitted masonry wall have been critically reviewed. Firstly, a detailed collection of several experimental tests using different
18 textile reinforced mortar and/or fiber reinforced mortar has been conducted. Special focus has been given to the test set-up and
19 load configuration type adopted for experiments. Subsequently, several modelling techniques have been treated in order to detect
20 the best approach simulating the interaction between reinforcement system and masonry ranging from macro and micro
21 modelling, concentrated and diffused plasticity model and diverse constitutive laws.

22 Finally, an overview of some original experimental outcomes from laboratory tests is presented. This results will play a major
23 role in for the validation of the numerical models for the prediction of the shear strength and the ductile behavior of reinforced
24 masonry that will be developed in a further step of this research.

25 © 2023 The Authors. Published by Elsevier B.V.

26 This is an open access article under the CC BY-NC-ND license (<https://creativecommons.org/licenses/by-nc-nd/4.0>)

1 Peer-review under responsibility of the scientific committee of the XIX ANIDIS Conference, Seismic Engineering in Italy.

* Corresponding author. Tel.: +39 3342556189.
E-mail address: raffaele.cucuzza@polito.it

2 *Keywords:* Review, retrofitting, masonry, textile reinforced mortar, fiber reinforced concrete, experimental investigations

3 **1. Introduction**

4 Aspects related to the modeling of masonry structures are of particular interest, both for the professional activity of
5 the engineer and for research (see e.g. Ferretti et al. 2021 and 2022). Several review papers or entire book chapters
6 emphasized the crucial role played by this topic into the structural engineering field, as reported by Beyer et al.
7 (2022) and Sarhosis et al. (2016). In the last decade, several retrofitting techniques, as Fiber reinforced polymer
8 (FRP) or textile reinforced mortar (TRM), became widespread and received special attention by engineers (see e.g.
9 Bertolesi et al. 2020, Formisano et al. 2021 and Faconi et al. 2016). While the former intends to make use of
10 simplified but reasonably accurate models, detailed modeling is still necessary for the timely evaluation of the
11 behavior of complex structures. In this respect, Cattari et al. (2021) provided an overview of the nonlinear modeling
12 considerations for assessing the seismic response of unreinforced masonry structures, with particular emphasis on
13 the effects that questioning modeling decisions might have on the outcomes of models considering extremely
14 complex architectural configurations. In fact, numerical models are now the only instruments considered to be
15 sufficiently effective to facilitate the seismic assessment of existing buildings, according to the specialized technical
16 community. The study discusses many methods, from the widely used Equivalent Frame approach to more
17 sophisticated methods including 2D and 3D Finite Element processes based on continuous, discrete, and micro-
18 mechanical approaches. They drew attention to many potential future advances for various simulation levels, such as
19 equivalent frame models. Additionally, a few challenging problems that are typical of the execution of nonlinear
20 time history studies were highlighted, such as the ability to simulate the cyclic response or the capacity to accurately
21 reproduce energy dissipation that is specially connected to ductility. Castellazzi et al. (2022) presented a comparison
22 of the outcomes of nonlinear static analysis performed on a masonry building using various programs that operate in
23 the fields of continuum and discrete macroelement modeling. The building was modeled after a real school that had
24 been damaged in the Central Italy earthquake in August 2016. With regard to the dispersion of the results and to the
25 potential consequences in the professional sector, the results provided some insights on the employment of
26 continuum and discrete-macroelement modeling.

27 Within research studies which associating experimental and numerical approaches to deep the structural behavior of
28 masonry elements, an experimental research on the mechanical performance of retrofitted brick masonry walls
29 under an in-plane cyclic shear test was presented by Garcia-Ramonda et al. in (2022). Unreinforced and retrofitted
30 with Basalt Textile Reinforced Mortar configurations of the specimens were tested. The examination of the
31 reinforced walls put through shear compression tests also made use of a sophisticated computational model. As a
32 continuous nonlinear homogeneous macromodel, the brickwork was modeled. The capacity of the model to predict
33 the in-plane behavior of retrofitted brick masonry walls was examined by comparing the numerical results with the
34 experimental results ones. Salsavilca et al. (2020) examined the behavior of the link between the composite layer
35 and the substrate given by a Peruvian masonry, when structural element were retrofitted by Steel Reinforced Grout.
36 Additionally, a characterization of the retrofit materials using compression tests on the mortar and direct tensile tests
37 on the fiber was reported. In order to create a cohesive material law, design bond parameters were also obtained
38 using an analytical model. Bellini et al. (2018) have provided an experimental campaign and a numerical analysis
39 devoted to the research of the out-of-plane behavior of masonry walls reinforced with Fiber Reinforced
40 Cementitious Matrix. In order to examine the behavior of strengthened masonry walls under out-of-plane horizontal
41 activities, such as, for example, seismic actions, they discussed the failure modes and capacity of the strengthening
42 system. The outputs of nonlinear studies carried out on simplified finite element models of the walls were discussed
43 and compared with the results of the present study. In order to develop trustworthy code recommendations that
44 result in the safe design of reinforced masonry structures, a proper assessment of the flexural capacity of the
45 strengthened walls is necessary.

46 In recent years, several researchers have developed intensive laboratory work in order to investigate the actual

1 behavior of differently consolidated masonry elements.
2 Incerti et al. (2019) conducted an extensive experimental campaign to evaluate the efficacy of the same
3 strengthening technique when it was applied to two different masonry typologies. Four masonry samples made of
4 hydraulic lime-based mortar and clay bricks were put through various testing using the Flemish bond and header
5 bond textures. Benefits seen in the samples' capacity, shear stiffness, and ductility were examined in light of
6 variations in building typologies. Moreover, comparisons were made with the theoretical findings from the Italian
7 Guidelines CNR DT 200.
8 An experimental examination of the structural behavior of masonry walls strengthened with Textile Reinforced
9 Mortar to increase their in-plane shear strength and deformation capacity (ductility) was presented by Garcia-
10 Ramonda et al. (2020). Ten clay brick and lime mortar masonry samples retrofitted with three alternative
11 technologies were diagonally compressed tested as part of the experimental program. On the inner face of the wall,
12 continuous basalt Textile Reinforced Mortar, discrete bands of unidirectional steel Textile Reinforced Mortar, and
13 continuous basalt Textile Reinforced Mortar were used. On the outer face of the wall, bed joints structural
14 repointing was done with near-surface mounted helical stainless-steel bars. Testing of several specimens in both
15 their unreinforced and repaired configurations revealed an improved increase in shear resistance and ductility,
16 making them acceptable for seismic retrofitting and post-earthquake repair.
17 In a subsequent paper, Garcia-Ramonda et al. (2022) offered an experimental program on masonry walls consisting
18 of handmade solid clay brick and hydraulic lime mortar. Reversed cyclic shear compression tests were performed on
19 the specimens in a variety of configurations, including unreinforced, repaired and retrofitted by using Basalt Textile
20 Reinforced Mortar. According to the experimental findings, the suggested solutions for seismic retrofit and post-
21 earthquake restoration of existing masonry buildings increased resistance, ductility, and energy dissipation in
22 comparison to unreinforced masonry shear walls. Furthermore, they helped to clarify the failure mechanisms and
23 displacement capabilities of the behavior of masonry walls subjected to cyclic horizontal displacements.
24 For shear masonry walls formed of handmade solid clay brick and hydraulic lime mortar, Garcia-Ramonda et al.
25 (2022) proposed an experimental investigation on the usage of steel reinforced grout as an in-plane strengthening
26 solution. On reinforced walls made of sheets of low-density steel, cyclic shear compression tests were performed.
27 The retrofitting was applied in a strip arrangement to both faces of the walls. In terms of failure mechanism, load-
28 bearing capacity, energy dissipation, and ductility, the experimental program sought to investigate the impact of the
29 number of textile layers on the in-plane response of strengthened masonry walls.
30 There is no doubt that the existing literature is full of laboratory insights into both the actual behavior of masonry
31 components and the impact of various retrofitting methods. Parallel to this development, numerical simulation has
32 also advanced to satisfy the design and verification requirements of reinforced or unreinforced masonry projects.
33 Nevertheless, despite significant advancements, there are still some areas that require some research and
34 advancement. One of these is unquestionably the transition from complex nonlinear modelling of masonry parts in
35 simplified equivalent frame approach with and without retrofitting operations (see e.g. Cattari et al. 2021). The
36 element's cyclic reaction and the contribution that retrofitting measures make to ductility are still two specific
37 characteristics of difficult challenges.
38 The goal of this contribution is to increase knowledge in this field. In order to highlight the effort in term of ductility
39 with respect to the cyclic shear stress of Fiber Reinforced Cementitious Matrix or in the presence of axial
40 compression, some laboratory results will be presented specifically on brick-and-mortar specimens not reinforced
41 with Fiber Reinforced Cementitious Matrix.
42 These will serve as a prelude to the step in which the element's structural modeling through micromodeling will be
43 explored in order to define a comprehensive, rich, and generalized database. The latter will serve as a tool to
44 subsequently advance a model with concentrated elemental flexibility and retrofitting intervention.

45 **2. Experimental investigations on masonry with Fiber Reinforced Cementitious Matrix (FRCM)**

46 With the aim to understand the effectiveness of the specific retrofitting system on different masonry typologies,
47 three experimental campaigns will be described. N. 38 squared masonry panels were realized within the extended
48 experimental campaign. Two different masonry materials were investigated. Full bricks and tuff materials were
49 considered by using blocks and lime-based mortar to reproduce masonry textures typical of the Italian built heritage.
50 Specifically, N. 8, n.18 and n.12 samples for each masonry panel material were subjected to uniaxial compression

tests, diagonal compression tests and out-plane bending tests respectively with the aim to evaluate the efficiency of the strengthening system and the influence of the masonry quality on the shear and bending behavior of the samples. The masonry typologies on which this strengthening technique can be applied are extremely variable, it can be affected by the nature of the components, the characteristics of the mortar and those of the masonry material. For all these reasons, the considered experimental investigations can be assumed as representative of the most common masonry typology constructed by clay bricks or sandstone and hydraulic lime-based mortar (class M5). Mainly, two different type of glass fiber reinforcements “OLY WALL M15” were investigated in experimental tests. Details concerning geometric and mechanical properties of bricks, cementitious mortar adopted for masonry joints and type of the glass fiber reinforcement are reported in Figure 1. Moreover, The FRCM strengthening layout was realized by a bi-directional basalt grid, embedded within two mortar matrix layers (overall thickness of 30 mm) and applied symmetrically on both sides of the masonry panels with a distance from the edge equal to 20 mm in order to prevent early debonding phenomena, as described in Incerti et al. (2015). Cold-drawn Helicoidal, realized using steel inox “Oly Chain” connectors with a diameter of 8 mm and maximum tensile strength equal to 10.5 kN, were adopted for each sample, aiming to anchorage the reinforcement layouts on the two sides of the masonry panels. In Table 1 and 2, characteristics of brick and mortar specimens and tested fiber grid are reported respectively.

Table 1. Characteristics of brick and mortar specimens.

	Type	Dimensions [cm]	Gross Density [kg/m ³]	Compressive strength [MPa]	Bending strength [MPa]
Solid Brick	Fired-clay	12x25x5.5	1700	30	-
Tufo	Sand-stone	25x37x11	1250	4.4	-
Mortar	Pre-mixed lime-based (M5)	0.04x0.04x0.16 (prismatic specimens)	1900	5	2

Table 2. Characteristics of the tested Fiber grid and Mortar matrix applied to the masonry samples.

	Type	Gross Density [kg/m ³]	Compression strenght [kN]	Tensile strenght [kN]	Flexural strenght [MPa]	Elastic Modulus [GPa]
Fiber grid 250	OLY WALL - 250	0.25	-	1.34	-	61
Fiber grid 550	OLY WALL - 550	0.55	-	2.42	-	67
Mortar Matrix	Pre-mixed lime-based	1550	15	-	4	-

In conclusion, an overview of the mechanical tests conducted for each specimen is pointed out in Table 3. In the following section, the results derived by the experimental tests are provided and some comparisons are carried out.

Table 3. Overview of the mechanical tests included within experimental campaign .

Masonry typology	Compression test	ID sample	Diagonal compression test	ID sample	Out-plane bending test	ID sample
Unretrofitted	N.2 masonry panels with solid bricks (1.0x1.2x0.25 m ³)	M26	N.3 masonry panels with solid bricks (1.2x1.2x0.25 m ³)	M23	N.3 masonry panels with solid bricks (0.8x1.2x0.25 m ³)	M28
		M27		M24		M29
				M25		M30
	N.2 masonry panels with sand-stone (1.0x1.2x0.25 m ³)	T34	N.3 masonry panels with sand-stone (1.2x1.2x0.25 m ³)	T31	N.3 masonry panels with sand-stone (0.8x1.2x0.25 m ³)	T36
		T35		T32		T37
Retrofitted with Glass fiber 250 + Connectors	N.2 masonry panels with solid bricks (1.0x1.2x0.25 m ³)	M13R	N.3 masonry panels with solid bricks (1.2x1.2x0.25 m ³)	M1R	N.3 masonry panels with solid bricks (0.8x1.2x0.25 m ³)	M10R
		M2R		M4R		M14R
				M6R		M17R
	N.2 masonry panels with sand-stone (1.0x1.2x0.25 m ³)	T21R	N.3 masonry panels with sand-stone (1.2x1.2x0.25 m ³)	T3R	N.3 masonry panels with sand-stone (0.8x1.2x0.25 m ³)	T11R
		T22R		T5R		T19R
			T12R		T20R	
Retrofitted with Glass fiber 550 + Connectors	-	-	N.3 masonry panels with solid bricks (1.2x1.2x0.25 m ³)	M7R	-	-
				M9R		
				M15R		

		N.3 masonry panels with sand-stone (1.2x1.2x0.25 m ³)	T8R T16R T18R	
Total	8	18	12	

1

2 *2.1. Experimental investigations: uniaxial compression tests set-up and results*

3 N. 8 squared masonry panels were realized within the experimental campaign. For comparison reason, the
 4 experimental campaign included unretrofitted masonry panels for each typology mentioned-above. Details
 5 concerning the geometric properties of specimens are reported in Table 1 and Table 2. Simple compression tests
 6 were conducted adopting a force control approach with a loading rate of 2.0 kN/sec (UNI EN 1926:2007).
 7 Moreover, a neoprene layer, with a thickness of 1.0 cm, was applied on the application surface during the test in
 8 order to reduce friction phenomena acting on the upper side of the specimen. Therefore, the same procedure was
 9 conducted to the reinforced samples too aim at avoiding debonding phenomena due to the contact between the
 10 loading machine and the mortar matrix. Tests were conducted using displacement hydraulic controller MTS with a
 11 maximum capacity of 500 kN (see Figure 3). An imposed displacement rate equal to 0.01 mm/s was imposed to
 12 detect softening branch. Diagonal deformations were measured by linear potentiometers (tensile and compressive).
 13 The measurement instrumentation adopted consisted of:

- 14 • N.1 Pressure transducer HBM with maximum pressure of 500 bar;
- 15 • N.4 inductive transducer HBM for the vertical displacement between two target points on the steel
- 16 frame and two target points on the panel surface;
- 17 • An acquisition control unit interfaced to a PC.

18

19

20

21

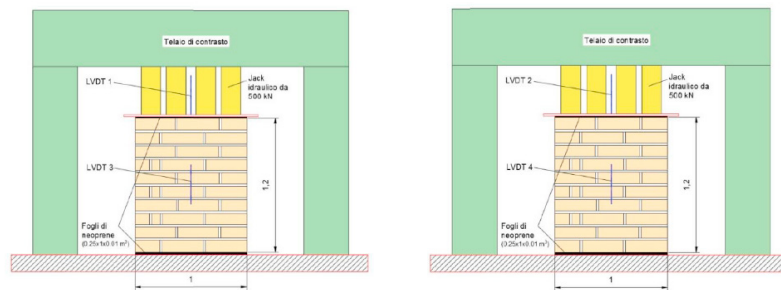
22

23

24

25

26



27 Fig. 1. Simple bending test set-up and measurement instrumentation adopted during the tests (dimensions are expressed in meters).

28 In Figure 2, it is reported a plot in which behaviors of “sandstone” and “solid brick” masonry panels, both
 29 unretrofitted and retrofitted with the two investigated type of reinforcement are depicted with the aim to observe the
 30 effectiveness of the strengthening systems and the influence of the specimens’ texture and material.

31

32

33

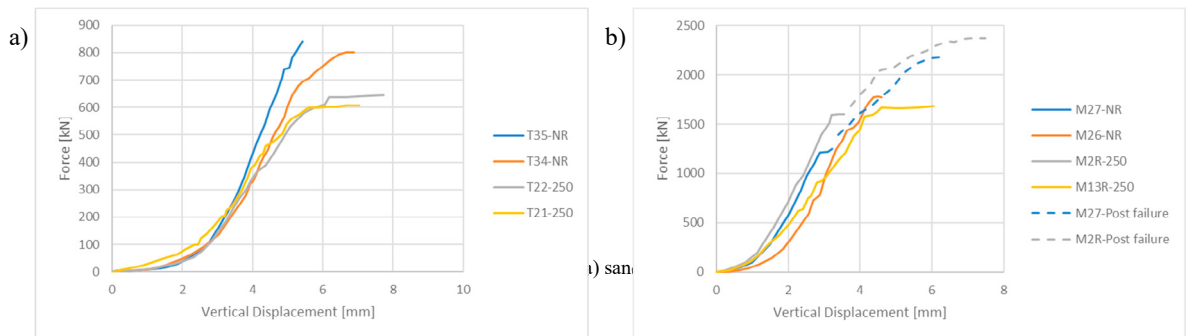
34

35

36

37

38



2.2. Experimental investigations: Diagonal compression tests set-up and results

N. 18 squared masonry panels were realized within the experimental campaign. For comparison reason, the experimental campaign included unretrofitted masonry panels for either “sandstone” and “solid brick” typology. Diagonal Compression tests were conducted adopting a force control approach with a loading rate of 1.0 kN/sec (ASTM E519-07, “Standard Test Method for Diagonal Tension in Masonry Assemblages”). The edges of the specimens are positioned at the level of steel angular profile (15x25 cm²) which are connected to a contrast steel frame as depicted in Figure 3.

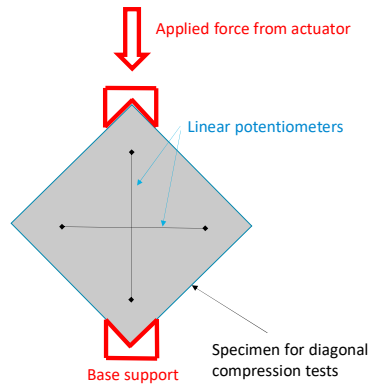


Fig. 3. Diagonal compression test setup

The same measurement instrumentation described in the previous section was adopted. However n.4 inductive transducers were placed along the compressed and tensioned diagonals of each specimen. Then, the samples were loaded in continuum using hydraulic actuators with a maximum capacity of 3000 kN. In Figure 4, results of the conducted test are provided in terms of shear force-shear deformation ($F-\gamma$) for both masonry typologies.

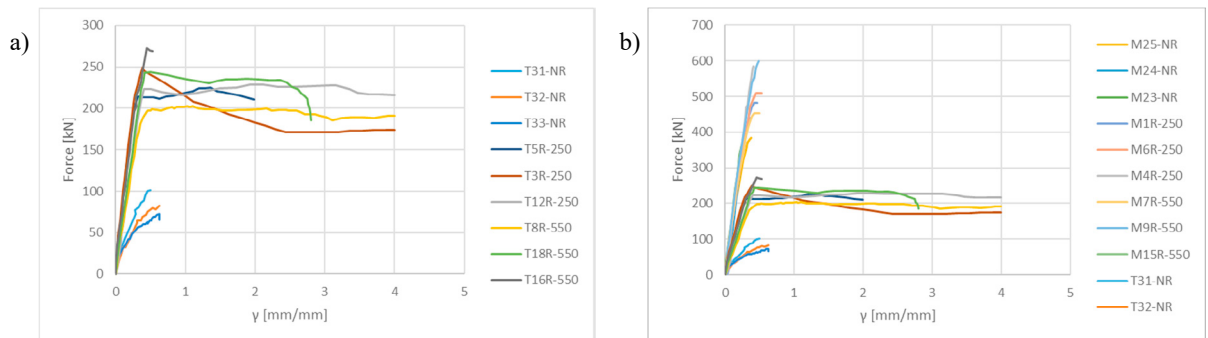


Fig. 4. Results of diagonal compression tests for (a) sandstone and (b) solid brick masonry panels

2.3. Experimental investigations: Out-plane bending tests set-up and results

N. 12 squared masonry panels were realized within the experimental campaign. For comparison reason, the experimental campaign included unretrofitted masonry panels for either “sandstone” and “solid brick” typologies. Out-plane bending tests were conducted adopting a force control approach with a loading rate of 0.3 kN/sec (EN 1052-2:2016). The bottom side of the panel was placed on a steel plate, edges of the specimens were contrasted by tubular steel beams by simulating cylindrical hinges during the loading phase and an actuator at the level of the middle height of the specimen was installed for transferred the out-plane bending to the structure. The same measurement instrumentation used for the previous cases within the experimental campaign was adopted with the

1 exception of the number of inductive transducers which were increased by n.1 unit with the aim to detect and
 2 monitoring the displacement points at 1/3 and 2/3 of both side of the panel and at the middle height in
 3 correspondence to the face in which actuator did not act (see e.g. Figure 5).

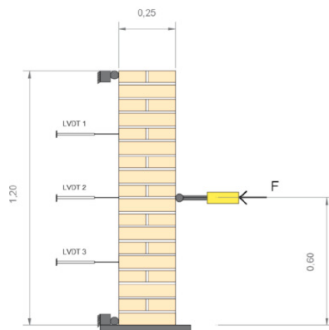


Fig. 5. Out-plane bending test set-up

16 Also for this case, in Figure 6 all the results of the experimental tests conducted by the authors are reported. With
 17 respect to the previous results obtained by bending and diagonal compression tests, specifically for this case, the
 18 outcomes derived by the experimental campaign were summarized in terms of maximum load achieved during the
 19 test, average of the maximum load considering specimens with the same type of reinforcement, texture and material.

20 Table 4. Results of Out-plane bending tests for sandstone and solid brick masonry panels. In the column dedicated to the average maximum
 21 loads, the coefficient of variation is reported within brackets.

ID Sample	Maximum load [kN]	Average maximum load [kN]	Masonry typology
T36	2.5	1.90 (28.0 %)	Unreinforced Sandstone
T37	1.44		
T38	1.77		
T11R	43.12	40.97 (5.34%)	Sandstone reinforced with 250 grid
T19R	38.74		
T20R	41.05		
M28	9.09	11.06 (17.45%)	Unreinforced Solid brick
M29	12.95		
M30	11.16		
M10R	41.85	41.01 (10.21%)	Solid brick reinforced with 250 grid
M14R	44.72		
M17R	36.47		

22 3. Conclusions

23 In this paper, an extensive literature review and the results of an extended experimental campaign were
 24 presented. Different masonry typologies with FRCM reinforcements were investigated with the aim to select the
 25 best retrofitting techniques for each scenario. Three different experimental tests were conducted. The outcomes of
 26 the diagonal compression test confirmed the efficiency of FRCM composites as a valuable strategy for improving
 27 the shear behavior of masonry panels and the global ductile behavior too. Specifically, from the comparisons
 28 between the unretrofitted specimens (T35-NR and T34-NR) and the reinforced ones (T22-250 and T21-250) a little
 29 improvement in term of ultimate deformation state was detected when the simple bending test was conducted.
 30 Similarly, reinforced solid brick panels (M2R-250 and M13R-250) received a negligible benefit from the
 31 reinforcement. Moreover, in the samples M2R and M27 when the maximum load equal to 600 kN was applied,

1 independently by the presence or not of the strengthening layout, a vertical crack split the specimen into two
2 different parts. The results derived from the compression diagonal tests confirmed the benefic effect of the
3 reinforcement and, with specific regard to simples retrofitted with 550 glass grid, a percentage increase equal to
4 179% and 40% was relieved with respect to the unreinforced specimens respectively. From diagonal compression
5 tests it was noticed that for sandstone and solid brick panels the FRCM reinforcement gave rise to a significant
6 increase of ultimate displacement of the order of about 800% in comparison to that of unreinforced specimens. For
7 both panel types the contribution given by the two different reinforcement types (fiber grids 250 and 550) was very
8 similar in terms of both ductility and ultimate strength. However, the maximum benefits deriving from FRCM
9 strengthening was observed in the out-plane bending tests. In fact, the highest value of maximum load was
10 recognized during these tests, for which the strength of the specimens was increased of 2056% and 270% with the
11 only addition of 250 glass grid reinforcement. For these specimens the results appear to be very reliable, since the
12 coefficient of variation was very small if compared to the unreinforced walls (5.34% instead of 28.00% for
13 sandstone panel and 10.21% instead of 17.45% for solid brick panel).

14 This first research preludes a subsequent analysis phase devoted to masonry modeling aiming at defining a
15 comprehensive, rich, and generalized database. It would serve to develop a concentrate plasticity model for new
16 equivalent frame modelling approaches.

17 References

- 18 Cattari, S., Calderoni, B., Calì, I., Camata, G., de Miranda, S., Magenes, G., ... & Sactta, A. (2021). Nonlinear modeling of the seismic response
19 of masonry structures: critical review and open issues towards engineering practice. *Bulletin of Earthquake Engineering*, 1-59.
20 DOI:10.1007/s10518-021-01263-1.
- 21 Castellazzi, G., Pantò, B., Occhipinti, G., Talledo, D. A., Berto, L., & Camata, G. (2022). A comparative study on a complex URM building: part
22 II. *Bulletin of Earthquake Engineering*, 20(4), 2159-2185. DOI:10.1007/s10518-021-01147-4
- 23 L. Garcia-Ramonda, L. Pelà, P. Roca, G. Camata, Experimental and numerical analysis of the cyclic in-plane behaviour of retrofitted masonry
24 walls, *Construction Pathology, Rehabilitation Technology and Heritage Management*, 2022, REHABEND 2022 Congress, September 13-16,
25 2022. Granada, Spain. *Construction and Building Materials*, 238, 117635. DOI:10.1016/j.engstruct.2020.111192
- 26 Bellini, A., Incerti, A., Bovo, M., & Mazzotti, C. (2018). Effectiveness of FRCM reinforcement applied to masonry walls subject to axial force
27 and out-of-plane loads evaluated by experimental and numerical studies. *International Journal of Architectural Heritage*, 12(3), 376-394. DOI:
28 10.1080/15583058.2017.1323246
- 29 Incerti, A., Tilocca, A. R., Ferretti, F., & Mazzotti, C. (2019). Influence of masonry texture on the shear strength of FRCM reinforced panels.
30 In *Structural analysis of historical constructions* (pp. 1623-1631). Springer, Cham. DOI:10.1007/978-3-319-99441-3_174
- 31 Garcia-Ramonda, L., Pelà, L., Roca, P., & Camata, G. (2020). In-plane shear behaviour by diagonal compression testing of brick masonry walls
32 strengthened with basalt and steel textile reinforced mortars. *Construction and Building Materials*, 240, 117905. DOI:
33 10.1016/j.conbuildmat.2019.117905
- 34 Garcia-Ramonda, L., Pelà, L., Roca, P., & Camata, G. (2022). Cyclic shear-compression testing of brick masonry walls repaired and retrofitted
35 with basalt textile reinforced mortar. *Composite Structures*, 283, 115068. DOI: 10.1016/j.compstruct.2021.115068
- 36 Garcia-Ramonda, L., Pelà, L., Roca, P., & Camata, G. (2022). Experimental cyclic behaviour of shear masonry walls reinforced with single and
37 double layered Steel Reinforced Grout. *Construction and Building Materials*, 320, 126053. DOI: 10.1016/j.conbuildmat.2021.126053
- 38 Incerti, A., Vasiliu, A., Ferracuti, B., & Mazzotti, C. (2015, December). Uni-Axial compressive tests on masonry columns confined by FRP and
39 FRCM. 12th International Symposium on Fiber Reinforced Polymers for Reinforced Concrete Structures, China, 14–16 December 2015.
- 40 Ferretti, F., & Mazzotti, C. (2021). FRCM/SRG strengthened masonry in diagonal compression: experimental results and analytical approach
41 proposal. *Construction and Building Materials*, 283, 122766. DOI: 10.1016/j.conbuildmat.2021.122766
- 42 Ferretti, F., Incerti, A., & Mazzotti, C. (2022). Efficiency of Strengthening Interventions on Stone Masonry Panels through Grout Injection and
43 FRCM. In *Key Engineering Materials* (Vol. 916, pp. 352-360). Trans Tech Publications Ltd. DOI: 10.4028/p-7i08im
- 44 Beyer, K., & Mangalathu, S. (2013). Review of strength models for masonry spandrels. *Bulletin of Earthquake Engineering*, 11(2), 521-542. DOI:
45 10.1007/s10518-012-9394-3
- 46 Sarhosis, V., De Santis, S., & de Felice, G. (2016). A review of experimental investigations and assessment methods for masonry arch
47 bridges. *Structure and Infrastructure Engineering*, 12(11), 1439-1464. DOI: 10.1080/15732479.2015.1136655
- 48 Bertolesi, E., Buitrago, M., Giordano, E., Calderon, P. A., Moragues, J. J., Clementi, F., & Adam, J. M. (2020). Effectiveness of textile reinforced
49 mortar (TRM) materials in preventing seismic-induced damage in a U-shaped masonry structure submitted to pseudo-dynamic
50 excitations. *Construction and Building Materials*, 248, 118532. DOI: /10.1016/j.conbuildmat.2020.118532
- 51 Formisano, A., Vaiano, G., & Petrucci, N. J. (2021, October). Hemp-FRP for Seismic Retrofitting of Existing Masonry Buildings.
52 In *International Conference on Protection of Historical Constructions* (pp. 402-417). Springer, Cham. DOI: 10.1007/978-3-030-90788-4_33
- 53 Facconi, L., Conforti, A., Minelli, F., Plizzari, G.A., 2015. Improving shear strength of unreinforced masonry walls by nano-reinforced fibrous
54 mortar coating. *Materials and Structures/Materiaux et Constructions*, 48 (8), pp. 2557-2574. DOI: 10.1617/s11527-014-0337-0. DOI:
55 10.1617/s11527-014-0337-0